

## Thermodynamics of Liquid Bi-Pb alloys – Experiment vs Modeling

Wang Jin<sup>1</sup>, Jin Weiliang<sup>1</sup>, Kou Qian<sup>1</sup>, Fang Xiaohong<sup>2</sup>, Xiao Saijun<sup>1</sup>, Zhang Jun<sup>1,\*</sup>

<sup>1</sup> School of Metallurgy Engineering, Anhui University of Technology, Maanshan, Anhui, China, 243002;

<sup>2</sup> School of Metallurgical and Ecological Engineering, University of Science & Technology Beijing, Haidian District, Beijing, China, 100083

\*E-mail: [zhjxsj@126.com](mailto:zhjxsj@126.com)

Received: 15 December 2019 / Accepted: 17 February 2020 / Published: 10 April 2020

---

Bi-Pb alloys are promising heat transfer fluid candidates for fast-neutron nuclear reactors and concentrating solar power systems. The thermodynamic properties of Bi-Pb alloys can be calculated effectively by using thermodynamic models. The molecular interaction volume model (MIVM) has been widely applied in research on the thermodynamics of metallic melt in recent years. In this paper, the thermodynamic properties of liquid Bi-Pb alloys were examined by using the electromotive force method. The partial and integral thermodynamic parameters of the system were calculated from the electromotive force. The activities and infinite dilution activity coefficient of Bi-Pb alloys at various temperatures were also calculated by the MIVM. A comparison between the experimental results and the theoretical results showed that the theoretical results are close to the experimental results and that the MIVM can be used for the thermodynamic calculation of lead-bismuth-based alloys.

---

**Keywords:** Bi-Pb alloys; Electromotive force method; Activity; Molecular interaction volume model

### 1. INTRODUCTION

Bi-Pb alloys are promising heat transfer fluid candidates for fast-neutron nuclear reactors and concentrating solar power systems, because they have low melting points and good thermophysical properties[1,2]. The investigation of the different properties of Bi-Pb alloys has attracted much attention[3~5] over the years because of their potential application in nuclear reactors.

In order to obtain the thermodynamic properties of multicomponent liquid alloys, reliable experiments are required[6~10]. However, it takes more time and needs more financial support for experimental study. Therefore, it is more convenient and economic to obtain the thermodynamic properties of alloys by model prediction. Barbin et al.[4] used thermodynamic modeling to investigate

the 45% Pb–55% Bi alloy equilibrium vaporization within a temperature range from 400 to 3000 K and pressures from  $10^{-3}$  to 100 atm. The vapor pressure, partial pressures of the vapor components, heat capacity, entropy, enthalpy, and thermal conductivity of Bi-Pb alloys relative to the temperature were determined. Adhikari et al.[11] used a simple statistical approach to study the thermodynamic, structural, transport and surface characteristics of liquid Bi-Pb alloys at a temperature of 700 K. The MIVM[12~14] has been studied and successfully applied in predicting the thermodynamic properties of binary and multicomponent liquid alloys in some investigations, which have indicated that the prediction ability of the MIVM is stable and reliable [15,16].

In this paper, electromotive force (EMF) measurements of liquid Bi-Pb alloys were performed. According to the EMF data, the thermodynamic parameters, such as the partial molar entropy of mixing, partial molar enthalpy of mixing and mixing Gibbs free energy, were determined. Thermodynamic data of Bi-Pb binary systems were calculated by employing the MIVM based on experimental results. A comparison between the calculated results and the theoretical results shows that the theoretical results are close to the experimental results.

## 2. EXPERIMENTAL AND THEORETICAL CALCULATION METHODS

### 2.1 Method of experimental measurement

In this paper, Bi-Pb alloys were selected as the research object, and NaCl-KCl molten salts were used as the electrolyte to measure the electromotive force of the battery of Bi-Pb alloys with different concentrations in the temperature range between 948 K and 1043 K to calculate its thermodynamic data.

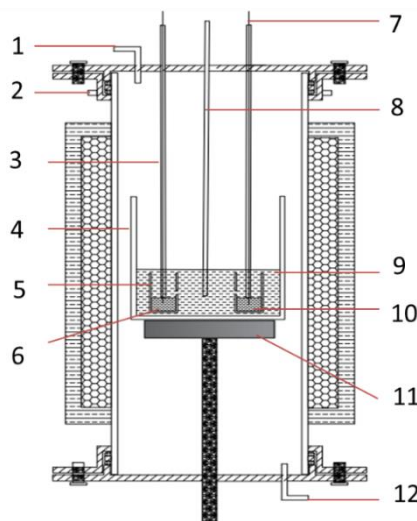


**Figure 1.** Schematic of the experimental setup for the electromotive force measurements. (1) argon gas inlet, (2) cooling system, (3) corundum tube ( $\Phi 6$  mm), (4) corundum crucible ( $\Phi 50$  mm), (5) corundum crucible ( $\Phi 9$  mm), (6) Pb (99.99%), (7) tungsten wire ( $\Phi 1$  mm), (8) thermocouple, (9) molten NaCl-KCl-PbCl<sub>2</sub> salts, (10) liquid Bi-Pb alloys, (11) graphite pallet, and (12) argon gas outlet.

Electrode concentration cells of the following type were used (n=2):

Pb (liquid)/PbCl<sub>2</sub> in NaCl-KCl/Bi-Pb (liquid)

With Bi-Pb alloys as the working electrode and pure lead as the reference electrode (RE), a reversible galvanic cell was assembled with NaCl-KCl-PbCl<sub>2</sub> molten salt as the electrolyte. The experimental device is shown in Fig. 1. The corundum crucible with Bi-Pb alloys and the liquid electrolyte were placed on the bottom of the larger corundum crucible and supported by a graphite pallet. Tungsten wire was used as the conducting wire, protected by a corundum tube. The inert atmosphere inside the resistance furnace could be maintained by introducing high-purity argon.

The experimental materials employed were all of high purity (> 99.9 wt%). After 1 hour of constant temperature at each temperature, each group of data was tested for 600 seconds. The Nernst equation converted the cell electromotive force into the activity of the alloy components. Because the use of the electromotive force cell method to investigate alloy solutions is a standard procedure, the experimental procedures are not described here.

### 2.2 Theoretical calculation by MIVM

Tao proposed the MIVM in 2000[12], which was based on the free volume theory and the lattice theory. The partition function of pure liquids and their mixtures was obtained, and a thermodynamic model of a new liquid alloy system was established. For the i-j binary liquid alloy, the molar excess Gibbs free energy is expressed as:

$$\frac{G_m^E}{RT} = X_i \ln \left( \frac{V_{mi}}{X_i V_{mi} + X_j V_{mj} B_{ji}} \right) + X_j \ln \left( \frac{V_{mj}}{X_j V_{mj} + X_i V_{mi} B_{ij}} \right) - \frac{X_i X_j}{2} \left( \frac{Z_i B_{ji} \ln B_{ji}}{X_i + X_j B_{ji}} + \frac{Z_j B_{ij} \ln B_{ij}}{X_j + X_i B_{ij}} \right) \quad (1)$$

where  $x_i$  and  $x_j$  represent the mole fractions of pure liquids i and j, respectively;  $V_{mi}$  and  $V_{mj}$  represent the molar volumes of pure liquids i and j, respectively;  $B_{ij}$  and  $B_{ji}$  represent the potential energy interaction parameters of i and j; and  $Z_i$  and  $Z_j$  represent the nearest neighbor number or first coordination number.

The activity coefficients of components i and j can be expressed as:

$$\ln \gamma_i = \ln \left( \frac{V_{mi}}{X_i V_{mi} + X_j V_{mj} B_{ji}} \right) + X_j \left( \frac{V_{mj} B_{ji}}{X_i V_{mi} + X_j V_{mj} B_{ji}} - \frac{V_{mi} B_{ij}}{X_j V_{mj} + X_i V_{mi} B_{ij}} \right) - \frac{X_j^2}{2} \left( \frac{Z_i B_{ji}^2 \ln B_{ji}}{(X_i + X_j B_{ji})^2} + \frac{Z_j B_{ij} \ln B_{ij}}{(X_j + X_i B_{ij})^2} \right) \quad (2)$$

$$\ln \gamma_j = \ln \left( \frac{V_{mj}}{X_j V_{mj} + X_i V_{mi} B_{ij}} \right) - X_i \left( \frac{V_{mj} B_{ji}}{X_i V_{mi} + X_j V_{mj} B_{ji}} - \frac{V_{mi} B_{ij}}{X_j V_{mj} + X_i V_{mi} B_{ij}} \right) - \frac{X_i^2}{2} \left( \frac{Z_i B_{ij}^2 \ln B_{ij}}{(X_j + X_i B_{ij})^2} + \frac{Z_j B_{ji} \ln B_{ji}}{(X_i + X_j B_{ji})^2} \right) \quad (3)$$

For a binary system i – j, its expressions of two infinite dilute activity coefficients  $\gamma_i^\infty$  and  $\ln \gamma_j^\infty$  can be derived from Eq. (2) and (3) when  $x_i$  or  $x_j$  approaches zero, respectively.

$$\ln \gamma_i^\infty = 1 - \ln \left( \frac{V_{mj} B_{ji}}{V_{mi}} \right) - \frac{V_{mi} B_{ij}}{V_{mj}} - \frac{1}{2} (Z_i \ln B_{ji} + Z_j B_{ij} \ln B_{ij}) \quad (4)$$

$$\ln \gamma_j^\infty = 1 - \ln \left( \frac{V_{mi} B_{ij}}{V_{mj}} \right) - \frac{V_{mj} B_{ji}}{V_{mi}} - \frac{1}{2} (Z_j \ln B_{ij} + Z_i B_{ji} \ln B_{ji}) \quad (5)$$

$B_{ij}$  and  $B_{ji}$  are respectively defined by Eq. (6) and (7).

$$B_{ij} = \exp \left[ -\frac{\epsilon_{ij} - \epsilon_{jj}}{kT} \right] \quad (6)$$

$$B_{ji} = \exp\left[-\frac{\varepsilon_{ji} - \varepsilon_{ii}}{kT}\right] \quad (7)$$

where  $\varepsilon_{ii}$ ,  $\varepsilon_{jj}$  and  $\varepsilon_{ji}$  are the i-j, j-j and i-j pair-potential energies, respectively, with  $\varepsilon_{ji} = \varepsilon_{ij}$ ,  $k$  is the Boltzmann constant and  $T$  is the temperature in Kelvin. In this paper,  $B_{ij}$  and  $B_{ji}$  are obtained by regression analysis of the experimental data.

### 3. RESULTS AND DISCUSSION

The average EMF measured in the experiment is shown in Table 1. When the activity of lead is the standard state of lead in liquid metal, the formula for calculating the activity is as shown in formula (8).

$$\ln a_{Pb} = -\frac{nF}{RT} E \quad (8)$$

In formula (8),  $n$  is the number of transferred electrons, and in this experiment,  $n$  is 2.  $F$  is the Faraday constant.  $E$  is the electromotive force,  $T$  is the temperature and  $a_{Pb}$  is the activity of lead.

**Table 1.** Experimental results of the EMF measurements and activities of lead in the Bi-Pb system

$x_{Pb}$	948 K		968 K		988 K		1018 K		1043 K	
	E(mV)	$a_{Pb}$								
0.098	119.21	0.054	120.84	0.055	123.63	0.055	126.21	0.056	128.84	0.057
0.202	82.66	0.132	83.34	0.136	86.92	0.130	88.92	0.132	89.34	0.137
0.298	64.26	0.207	65.02	0.210	66.06	0.212	67.43	0.215	68.83	0.216
0.402	47.33	0.314	48.4	0.313	49.72	0.311	50.44	0.317	51.33	0.319
0.505	33.03	0.445	34.06	0.442	34.7	0.443	35.56	0.444	38.06	0.429
0.602	24.35	0.551	24.83	0.551	25.47	0.550	26.05	0.552	26.51	0.554
0.700	16.27	0.671	16.55	0.672	16.83	0.673	17.33	0.674	18.01	0.670
0.792	9.26	0.797	9.76	0.791	10.3	0.785	10.84	0.781	11.37	0.776
0.893	4.97	0.885	5.15	0.884	5.5	0.879	5.69	0.878	5.84	0.878

The activities of bismuth were calculated by Gibbs-Duhem integration. The data are also shown in Table 2. All the activities of bismuth and lead indicate that this system deviates negatively from Raoult's law.

Table 3 shows the activities of bismuth at 948 K along with the corresponding data from the earlier EMF studies of Moldovan[17] and Mikula[18]. It was observed that there are good agreements between the present results and the earlier ones.

**Table 2.** Activities of bismuth in the Bi-Pb system

$x_{Pb}$	$a_{Bi}$ (948 K)	$a_{Bi}$ (968 K)	$a_{Bi}$ (988 K)	$a_{Bi}$ (1018 K)	$a_{Bi}$ (1043 K)
0.098	0.896	0.896	0.896	0.896	0.896
0.202	0.777	0.778	0.776	0.776	0.778
0.298	0.658	0.659	0.660	0.662	0.663
0.402	0.535	0.534	0.532	0.537	0.539
0.505	0.434	0.431	0.431	0.433	0.417
0.602	0.325	0.325	0.323	0.327	0.330
0.700	0.239	0.241	0.243	0.243	0.236
0.792	0.228	0.205	0.183	0.170	0.156
0.893	0.059	0.052	0.035	0.034	0.033

**Table 3.** Activities of bismuth in the Bi-Pb system at 948 K

$x_{pb}$	$a_{pb}$	$x_{pb}$ [17]	$a_{pb}$ [17]	$x_{pb}$ [18]	$a_{pb}$ [18]
0.098	0.0540	0.109	0.0633	0.1	0.0589
0.202	0.1321	0.201	0.1269	0.207	0.1329
0.298	0.2073	0.320	0.2071	0.296	0.2095
0.402	0.3138	0.403	0.3146	0.397	0.3097
0.505	0.4454	0.510	0.4347	0.497	0.4233
0.602	0.5509	0.612	0.5582	0.599	0.5480
0.700	0.6714	0.724	0.7032	0.699	0.6483
0.792	0.7971	0.850	0.8234	0.801	0.7898
0.893	0.8854	0.906	0.9007	0.903	0.8991

The linear relationship between the EMF and temperature at different concentrations was obtained by regression analysis of the EMF measurements at different temperatures and concentrations shown in Table 1, as presented in Table 4. At the same time, the change in the partial molar entropy of Pb,  $\Delta \bar{S}_{Pb}$ , was calculated according to the temperature coefficient of the EMF.

$$\Delta \bar{S}_{Pb} = nF \frac{dE}{dT} \tag{9}$$

The partial thermodynamic functions of the lead and bismuth in the alloy were calculated by the following equations.

$$\Delta \bar{G}_{Pb} = RT \ln a_{Pb} = -nFE \tag{10}$$

$$\Delta \bar{H}_{Pb} = \Delta \bar{G}_{Pb} + T \Delta \bar{S}_{Pb} = -nF \left( E - T \frac{dE}{dT} \right) \tag{11}$$

$$\Delta \bar{G}_{Bi} = RT \ln a_{Bi} \tag{12}$$

$$\Delta \bar{S}_{Bi} = - \frac{d\bar{G}_{Bi}}{dT} \tag{13}$$

$$\Delta \bar{H}_{Bi} = \Delta \bar{G}_{Bi} + T \Delta \bar{S}_{Bi} \tag{14}$$

To calculate the integral molar characteristics of the mixing of components of the Bi-Pb system, we used the following equation.

$$\Delta G = n_{Bi} \Delta \bar{G}_{Bi} + n_{Pb} \Delta \bar{G}_{Pb} \tag{15}$$

$\Delta \bar{G}_{Pb}$  and  $\Delta \bar{G}_{Bi}$  are the partial molar mixing Gibbs free energies of lead and bismuth. The partial molar mixing enthalpies of lead and bismuth are  $\Delta \bar{H}_{Pb}$  and  $\Delta \bar{H}_{Bi}$ , respectively.  $\Delta \bar{S}_{Bi}$  is the partial molar mixing entropy of bismuth.  $\Delta G$  is the total mixing Gibbs free energy of Bi-Pb alloys. The thermodynamic functions of Bi-Pb alloys calculated at 948 K are shown in Table 5.

**Table 4.** The relationship between the EMF and temperature at different concentrations between 948 K and 1043 K

$x_{Pb}$	E=a+bT (K)	$\Delta \bar{S}_{Pb}$ (J.mol <sup>-1</sup> .K <sup>-1</sup> )
0.098	0.1024T+22.109	19763.2
0.202	0.0737T+13.296	14224.1
0.298	0.0482T+18.425	9302.6
0.402	0.0412T+8.517	7951.6
0.505	0.0484T-12.967	9341.2
0.602	0.0229T+2.6886	4419.7
0.7	0.0179T-0.7562	3454.7
0.792	0.0219T-11.489	4226.7
0.893	0.0094T-3.8751	1814.2

**Table 5.** Thermodynamic functions of bismuth-lead binary alloy mixing calculated at 948 K

$x_{pb}$	$\Delta \bar{G}_{Pb}$ (J.mol <sup>-1</sup> )	$\Delta \bar{S}_{Pb}$ (J.mol <sup>-1</sup> .K <sup>-1</sup> )	$\Delta \bar{H}_{Pb}$ (J.mol <sup>-1</sup> )	$\Delta \bar{G}_{Bi}$ (J.mol <sup>-1</sup> )	$\Delta \bar{G}$ (J.mol <sup>-1</sup> )
0.098	-23007.5	19763.2	13317152.5	-868.4	-3038.0
0.202	-15953.4	14224.1	9585314.1	-1992.9	-4812.9
0.298	-12402.2	9302.6	6266852.8	-3304.1	-6015.3
0.402	-9134.7	7951.6	5358195.3	-4934.6	-6623.1
0.505	-6374.8	9341.2	6298935.2	-6572.8	-6472.8
0.602	-4699.6	4419.7	2978598.0	-8862.0	-6356.2
0.7	-3140.1	3454.7	2328782.4	-11280.1	-5582.1
0.792	-1787.2	4226.7	2851235.3	-11639.7	-3836.5
0.893	-959.2	1814.2	1223625.8	-22299.2	-3242.6

The relationship between the total free energy and the concentration of lead and bismuth in the two alloy melts at different temperatures is shown in Fig. 2.

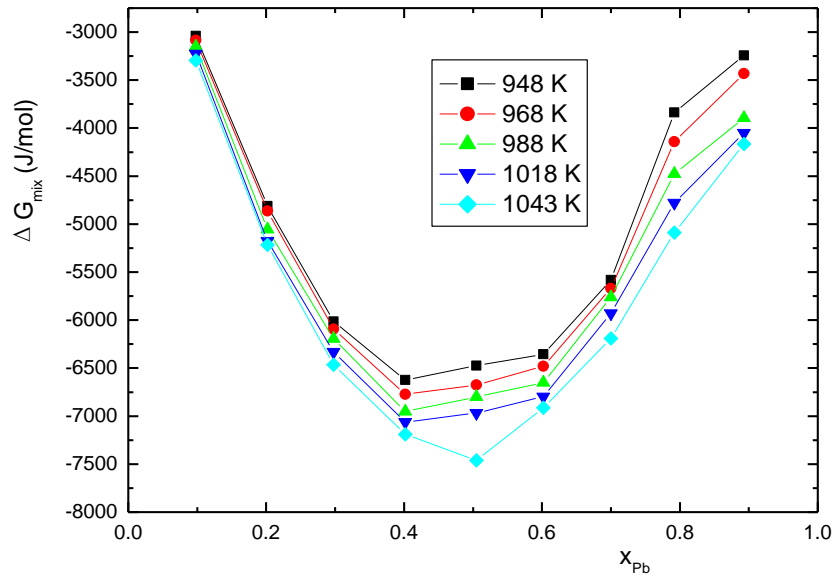


**Figure 2.** Relationship between total Gibbs free energy and concentration of lead and bismuth in two alloy melts at different temperatures.

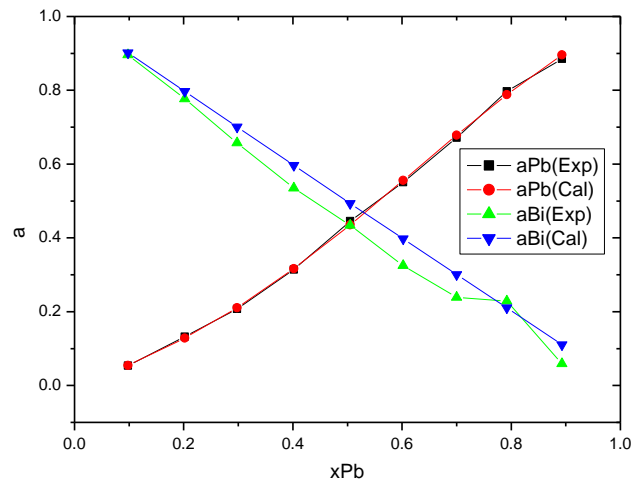
According to the calculation method provided in Section 2.2, the thermodynamic data of lead-bismuth binary alloys are calculated by using the MIVM and compared with the experimental results to evaluate the accuracy of the MIVM.

Table 6 shows the parameters needed for calculating the melt activity of lead-bismuth binary alloys by the MIVM.  $B_{ij}$  and  $B_{ji}$  are obtained by regression of the activity data measured in this experiment.

**Table 6.** Table of parameters required for calculating the activity of Bi-Pb alloys based on the MIVM[19,20]

T/K	$V_{mPb}$	$V_{mBi}$	$Z_{Pb}$	$Z_{Bi}$	$B_{ij}$	$B_{ji}$
948	20.2372	21.7832	8.6585	7.9343	0.4727	1.6293
968	20.2853	21.8318	8.6285	7.8977	0.4927	1.6096
988	20.3334	21.8805	8.5989	7.8623	0.4839	1.6198
1018	20.4055	21.9535	8.5553	7.8107	0.4935	1.6052
1043	20.4657	22.0144	8.5199	7.7691	1.1271	1.0051

The activity values of lead and bismuth calculated by the MIVM are compared with the experimental values at 948 K, as shown in Fig. 3.



**Figure 3.** Comparison between the experimental values of Pb and Bi activity with the MIVM values in the Bi-Pb system at 948 K.

From Fig. 3, we can see that the calculated activity values of the molecular interaction volume are close to the experimental measurements. This outcome is the same at 968 K, 988 K, 1018 K and 1043 K. The average relative error ( $S_i$ ) and standard deviation ( $S_i^*$ ) are as follows, respectively.

$$S_i = \pm \left( \frac{100}{t} \right) \sum_{i=1}^t \left| \frac{a_{i,exp} - a_{i,pre}}{a_{i,exp}} \right| \tag{16}$$

$$S_i^* = \pm \sqrt{\left[ \frac{1}{t} \sum_{i=1}^t (a_{i,exp} - a_{i,pre})^2 \right]} \tag{17}$$

where  $a_{i,exp}$  and  $a_{i,pre}$  are the calculated experimental results and predicted values of the activity of component i in the system, respectively, and t is the amount of experimental data. The comparative error analysis between the calculated and experimental values of the MIVM at various temperatures is demonstrated in Table 7.

**Table 7.** Error analysis of activity calculations at various temperatures

T / K	$S_{Pb, \%}$	$S_{Pb}^*$	$S_{Bi, \%}$	$S_{Bi}^*$
948	±1.5033	±0.0066	±19.7969	±0.0492
968	±1.316	±0.0055	±9.4547	±0.0281
988	±0.8942	±0.0063	±15.5854	±0.025
1018	±0.7373	±0.0061	±15.8041	±0.0215
1043	±1.1021	±0.0052	±13.3225	±0.0144

Table 7 shows that all average relative errors ( $S_i$ ) are between  $\pm 0.7373\%$  and  $\pm 19.7969\%$  and that the standard deviations ( $S_i^*$ ) are from  $\pm 0.0052$  to  $\pm 0.0492$ , predicted by the MIVM. The errors are small. These results show that the MIVM is an effective model for predicting the activities of Bi-Pb alloys at different temperatures.

In addition, according to the calculation method presented in Section 2.2, the infinite dilution activity coefficients of Bi-Pb alloys at different temperatures are calculated based on the MIVM. The results are shown in Table 8, and compared with those in Ref [9].

**Table 8.** Infinite dilute activity coefficient of binary Bi-Pb alloys based on the MIVM

T/K	$\gamma_{\text{Pb}}^{\infty}$ (MIVM)	$\gamma_{\text{Pb}}^{\infty}$ [9]	$\gamma_{\text{Bi}}^{\infty}$ (MIVM)	$\gamma_{\text{Bi}}^{\infty}$ [9]
948	0.4921	0.4794	0.6693	0.5153
968	0.5048	0.4852	0.6306	0.5207
988	0.4975	0.4908	0.6381	0.5260
1018	0.5126	0.4989	0.6446	0.5336
1043	0.5110	0.5054	0.5410	0.5397

From Table 8, we can see that the calculated values of  $\gamma_{\text{Pb}}^{\infty}$  and  $\gamma_{\text{Bi}}^{\infty}$  based on the MIVM are relatively close to the reported values in Ref [9]. These results show that the MIVM is an effective model for predicting the infinite dilute activity coefficients of Bi-Pb alloys at different temperatures.

The relationships between the infinite dilution activity coefficients calculated based on the MIVM and temperature are shown in formulas (18) and (19), obtained by regression analysis.

$$\ln \gamma_{\text{Pb}}^{\infty} = -0.438 - 246/T \quad (18)$$

$$\ln \gamma_{\text{Bi}}^{\infty} = -2.153 + 1667/T \quad (19)$$

According to the infinite dilute activity coefficients provided by formulas (18) and (19), we can use the molecular interaction volume model to calculate the activity and other thermodynamic quantities of Bi-Pb alloys.

#### 4. CONCLUSIONS

(1) In this paper, Bi-Pb alloys were selected as the research object, and the battery electromotive force of different components of Bi-Pb alloys between 948 K and 1043 K were studied using NaCl-KCl-PbCl<sub>2</sub> molten salt as the electrolyte. The activity and the partial and integral thermodynamic characteristics of Bi-Pb alloys were calculated according to thermodynamic theory. The experimental results indicate that the Bi-Pb alloy system deviates negatively from Raoult's law;

(2) The molecular interaction volume model (MIVM) was employed to calculate the activities and infinite dilution activity coefficients of Bi-Pb alloys, and it can be concluded that the relationship between the infinite dilution activity coefficients of lead and bismuth and the temperature

is  $\ln \gamma_{Pb^\infty} = -0.438 - 246/T$  and  $\ln \gamma_{Bi^\infty} = -2.153 + 1667/T$ , respectively, between 948 K and 1043 K.

#### ACKNOWLEDGEMENTS

The authors are grateful for the financial support from National Natural Science Foundation of China, Project (51404001) and Anhui Province overseas scholars innovation project funding program.

#### References

1. A. M. Azad. *J. Nucl. Mater.*, 341 (2005) 45.
2. M. P. Popović, D. L. Olmsted, A. M. Bolind, M. Asta, S. Sohn, J. Schroers, R. Shao and P. Hosemann. *Mater. Des.*, 159 (2018) 240.
3. N. Barbin, D. Terentiev, S. Alexeev and T. Barbina. *Comput. Mater. Sci.*, 66 (2013) 28.
4. N. M. Barbin, I. V. Tikina and D. I. Terent'Ev. *High Temp.*, 55 (2017) 506.
5. N. Barbin, D. Terentiev, S. Alexeev and T. Barbina. *Phys. Chem. Liq.*, 55 (2017) 100.
6. R. J. Fruehan. *Metall. Trans.*, 2 (1971) 1213.
7. R. Prasad, V. Venugopal and D. D. Sood. *J. Chem. Thermodyn.*, 9 (1977) 593.
8. K. Okajima and H. Sakao. *Trans. JIM*, 29 (1988) 469.
9. P. Taskinen and O. Teppo. *Scand. J. Metall.*, 21 (1992) 181.
10. Yu. R. Khalimullina, Yu. P. Zaikov, P. A. Arkhipov, V. V. Ashikhin, G. V. Skopov, A. S. Kholkina and N. G. Molchanova. *Russ J Non-Ferr Met.*, 52 (2011) 197.
11. P. Dahal, N. K. Rajbansi and D. Adhikari. *J. Mol. Liq.*, 191 (2014) 151.
12. D. P. Tao. *Thermochim. Acta*, 363 (2000) 105.
13. D. P. Tao. *Metall. Mater. Trans. B*, 47 (2016) 1.
14. D. P. Tao. *Metall. Mater. Trans. B*, 45 (2014) 142.
15. M.N. Jocelyn, P. Sophie, K. Hojong, L.S. Brian and R.S. Donald. *Electrochim. Acta*, 91 (2013) 293.
16. S. Poizeau and D. R. Sadoway. *J. Am. Chem. Soc.*, 135 (2013) 8260.
17. P. Moldovan. *Bull. Inst. Politechn. Bucuresti, Ser. Chim-Metal.*, 39 (1977) 107.
18. A. Mikula. *Monatsh. Chem.*, 117 (1986) 1379.
19. T. Iida and R. I. L. Guthrie. *The physical properties of liquid metals*, Clarendon Press, (1988) Oxford, United States.
20. G.D. Zhou. *Periodic Table of Elements*, Chemical Industry Press, (2006) Beijing, China.

© 2020 The Authors. Published by ESG ([www.electrochemsci.org](http://www.electrochemsci.org)). This article is an open access article distributed under the terms and conditions of the Creative Commons Attribution license (<http://creativecommons.org/licenses/by/4.0/>).